JOURNAL OF CATALYSIS **173,** 374–382 (1998)
ARTICLE NO. CA971924

Pd/SiC Catalysts

Characterization and Catalytic Activity for the Methane Total Oxidation

Ch. Méthivier,* B. Béguin,† M. Brun,* J. Massardier,*,[1] and J. C. Bertolini*

*Institut de Recherches sur la Catalyse—CNRS, conventionné à l'Université Claude Bernard Lyon 1, 2, avenue Albert Einstein, 69626 Villeubanne Cedex, France; and †Laboratoire d'Application de la Chimie à l'Environnement, Unité Mixte CNRS—Université Claude Bernard Lyon 1, 43 boulevard du 11 novembre 1918, 69626 Villeurbanne Cedex, France

Received June 6, 1997; revised September 12, 1997; accepted September 13, 1997

Silicon carbide, SiC, is a refractory material which shows a high thermal conductivity. Therefore, a better thermal stability of both the catalytic active phase and of the support for the SiC supported metallic catalysts can be expected for reactions occurring at high temperature and/or for highly exothermic reactions working with high turnover frequency. Various Pd based catalysts have been prepared by impregnation of a β-SiC support with Pd(II) acetylacetonate [$Pd(AcAc)_2$] and tested for the methane oxidation. The activity and thermal stability of the catalysts are depending on the process used for the $Pd(AcAc)_2$ decomposition on β-SiC. When the $Pd(AcAc)_2$ complex is decomposed under Ar atmosphere at 400°C the catalyst presents small metal particles homogeneous in size. But, they are strongly deactivated after ageing under an oxidizing mixture up to 800°C. The samples obtained after decomposition under O_2 at 350°C, further reduced under H_2, present larger particles and some formation of palladium silicide Pd_2Si. They are first less active, but they show only a slight deactivation after ageing under an oxidizing mixture up to 800°C. The direct decomposition of the catalytic precursor under H_2 leads to large Pd particles. As for the precedent catalyst, they deactivate only moderately after reaction at 800°C.

Key Words: **silicon carbide; palladium; methane oxidation.**

INTRODUCTION

In catalytic reactions, the materials used as supports of the active phases are generally insulators such as SiO_2, Al_2O_3, silica-alumina, and different zeolithic frameworks. These materials show a rather low thermal conductivity and, therefore, sintering of both metal and support occurs when they are used for highly exothermic reactions mainly if they are working with high turnover frequency (hydrogenation reactions) or/and for reactions occurring at high temperatures (hydrocarbon oxidation reactions). Such a sintering is accelerated by the presence of "hot spots." One way to rule out these disadvantages would be the use of ceramic materials having high thermal conductivity, which, up until today, still are not employed on a large scale. Nevertheless, some works have already been undertaken (1–5).

Briefly, three points of interest can be emphasized: (i) they show very good mechanical properties which give them important resistance to erosion and attrition, in addition to a high thermal stability; (ii) they present a higher thermal conductivity compared to the more conventional supports which could prevent the metal sintering; (iii) they are particularly inactive with respect to chemical reagents such as acids or bases. Therefore, the active phase can be easily reprocessed after simple acidic or basic treatments.

Among refractory materials, the thermal conductivity of silicon carbide, SiC (500 W/m · K for crystalline state, at room temperature) is close that of metals such as Ag or Cu (400–500 W/m · K).

The work reported here was devoted to the preparation and characterization of Pd/SiC catalysts. Their performances were monitored for a high temperature reaction, the oxidation of methane, the reaction for which Pd is active and selective, leading to clean combustion without NO or CO production.

EXPERIMENTAL

(a) The Supports

Two crystallographic forms of SiC are known: (i) the high temperature (>1500°C) hexagonal α-phase one which shows several polytypes, 4H, or 6H and (ii) the low temperature form (<1500°C) cubic β-phase (6). Whatever the crystallographic phase, they have a significant increase of the thermal conductivity both at room temperature and at higher temperatures (1000°C). Physical properties of SiC materials prepared by chemical vapor deposition (CVD) are given in Table 1, together with the corresponding values for silica and alumina.

[1] E-mail: massard@catalyse.univ-lyon1.fr.

0021-9517/98 $25.00

TABLE 1

Physical Characteristics of Massic SiC from CREE, NASA, Céramiques et Composites and Morton, in Comparison with Alumina and Silica

Samples	Manufacturer	M. Pt. (°C)	W. T. (°C)	Thermal conductivity (W/m°C) at RT	Thermal conductivity (W/m°C) at 1000°C	Lattice parameter (nm)
Hex. α-SiC	CREE	2600		490		a = 0.3081
(6H polytype)	NASA	2600		490		c = 1.512
	C & C		1800	180	40	
Cubic β-SiC	NASA			500		a = 0.436
	Morton	2700*		330	78	
SiO_2		1710	1200	1	2	
Al_2O_3		2050	1850	30	9	

Note. M. Pt., Melting point, or *, sublimation temperature. W. T., working temperature.

In this work we investigated "a priori" two SiC supports having respectively the high temperature hexagonal structure polytype 6H (from Goodfellow) and the low temperature cubic structure (from Nippon Carbide).

(b) Preparation of Catalysts

The low content of chemical anchoring sites (OH groups) of SiC refractory materials does not allow us to use the exchange method for the preparation of the supported metal catalysts. Therefore, the samples have been prepared by impregnation of SiC with the adequate amount of a Pd complex, Pd(II) bis acetylacetonate [$Pd(C_5H_7O_2)_2$] (99% from STREM), dissolved in toluene. Previous works at the IRC laboratory have shown that well-dispersed samples are obtained by such a mehod (7).

After evaporation of toluene and drying overnight at 80°C, the residue was either decomposed under argon at 400°C, under oxygen at 350°C, or under hydrogen flow at 300°C. After decomposition under oxygen an additional reduction under hydrogen flow at 300°C has to be carried out. In the following, we will refer to these three decomposition procedures as activation treatments.

(c) Characterization of Catalysts

The various catalysts were firstly characterized by H_2 chemisorption and with using electron microscopy (TEM); this was done with using a JEOL 2010 microscope working at 200 keV. Photoemission XPS measurements were made in complement on an ESCALAB 200R machine, from FISONS Instruments.

For H_2 chemisorption measurements, the reduced samples were first evacuated at the temperature of reduction and cooled under vacuum at room temperature. Hydrogen was then reintroduced and again evacuated. The samples were then heated (40 K/mn) and the thermodesorbed hydrogen measured by mass spectrometry. In this way, the results are not altered by the Pd hydride formation which is destroyed by the evacuation. The amount of adsorbed hydrogen is calculated from the H_2 TDS peaks areas. The calibration of the TDS peaks was performed by the H_2 uptake on a well-characterized Pd/SiO_2 sample, used as a standard, for which the dispersion—number of Pd atoms chemisorbing H_2/number of total Pd—is well known.

(d) Catalytic Experiments

The catalytic properties of the Pd/SiC samples were measured for the total oxidation of methane. The catalytic experiments were performed at atmospheric pressure in a gas flow reactor. The test reaction was carried out in an oxidizing mixture, O_2 (4%)/CH_4 (1%)/N_2 (95%), on 300 mg of catalyst spread on a sintered glass. The gas mixture was analyzed every 15 min by gas phase chromatography using both a TCD detector and a flame ionization detector. The hourly space velocity varied between 5000–6000 h^{-1}. The reaction was studied at increasing temperatures (1 K/mn) between 200 and 600°C. Only CO_2 and H_2O were formed in the course of the run. The methane conversion was measured as a function of the reaction temperatures for three states of the samples:

State 1. Previously activated samples are only prereduced at 300°C by H_2 before reaction and cooled at room temperature under N_2 flow.

State 2. Samples after a first "methane-oxygen reaction" up to 600°C and cooled under N_2.

State 3. Samples after ageing ($CH_4 + O_2$ up to 800°C during 3 h).

RESULTS

The crystallographic structure of the two considered SiC samples used as supports (having respectively the high temperature hexagonal structure polytype 6H, from

TABLE 2

Main Characteristics of the Studied α-SiC and β-SiC Powders

Sample	(BET) Surf. (m^2/g)	BE Si 2p (SiC) (eV)	BE Si 2p (SiO_2) (eV)	BE C 1s (SiC) (eV)	[SiC]/ [SiC + SiO_2]
α-SiC	1.5	100.2	103.3	282.2	0.84
β-SiC	17.1	100.2	Not detected	282.2	≈1

Goodfellow, and the low temperature cubic structure, from Nippon Carbide) was confirmed by analysis of their X-ray diffraction patterns, which show very narrow lines characteristic of well-crystallized samples.

Differences between the two samples have to be underlined:

(i) the BET area of the α-SiC phase purchased from Goodfellow is about one order of magnitude lower than that of the β-SiC issued from Nippon Carbide (Table 2).

(ii) the α-SiC is covered by a thin layer of silica (SiO_2) as it can be concluded from the analysis of the XPS spectra of Si 2p, C 1s, and O 1s recorded on the two supports (see Fig. 1 for the Si 2p and C 1s region).

In Table 2 the binding energies and their corresponding chemical states are given. Only one chemical state of silicon is observed on the β-SiC, with a Si 2p binding energy at 100.2 eV, as expected from reported data (8, 9), whereas the oxidized silicon form (namely at 103.3 eV for SiO_2) is detected on the α-SiC. Such a presence of oxidized silicon in the SiC surface region has been mentioned already even on well-defined crystalline samples (10–12). On the two samples, the binding energy of C 1s at 282.2 eV is characteristic of the chemical state of carbon in silicon carbide. However, there is a small peak at 284.5 eV on α-SiC due to some pollution-like carbon. From the [SiC]/[SiC + SiO_2] ratio, determined from XPS experiments and therefore characteristic of the mean composition of the outer layers, it can be concluded that the α-SiC is covered by a thin layer of SiO_2 (depth of ≈0.5 nm) and a little additionnal carbon. The β-SiC material can be considered as very clean in agreement with its very narrow Si 2p photopeak and a "quasi" stoichiometric Si/C ratio.

Taking into account the low value of the BET area of the α-SiC support and also the presence of a SiO_2 layer at its surface, the catalysis experiments were carried out preferentially using the β-SiC support.

The Pd content has been chosen to be near 1 wt%; such a value is sufficient to allow satisfying the physical characterization but not too large in order to obtain a rather good spreading of particles on such supports having low specific area. The metallic surface has been determined using H-adsorbed TPD and TEM observations. In our conditions of heating (40 K/mn), whatever the sample, the TPD spectra show one peak with a temperature maximum near 390 K. The data are given in Table 3, together with the results of TEM observations (Fig. 2). Depending on the activation treatments previously described, one gets catalysts having different characteristics. TEM observations clearly show that only the direct decomposition under an argon atmosphere leads to the formation of rather small particles. The disagreement between the particle size determination by H_2 chemisorption and TEM is due to the presence of carbon residues. This has been demonstrated on Pd/SiO_2

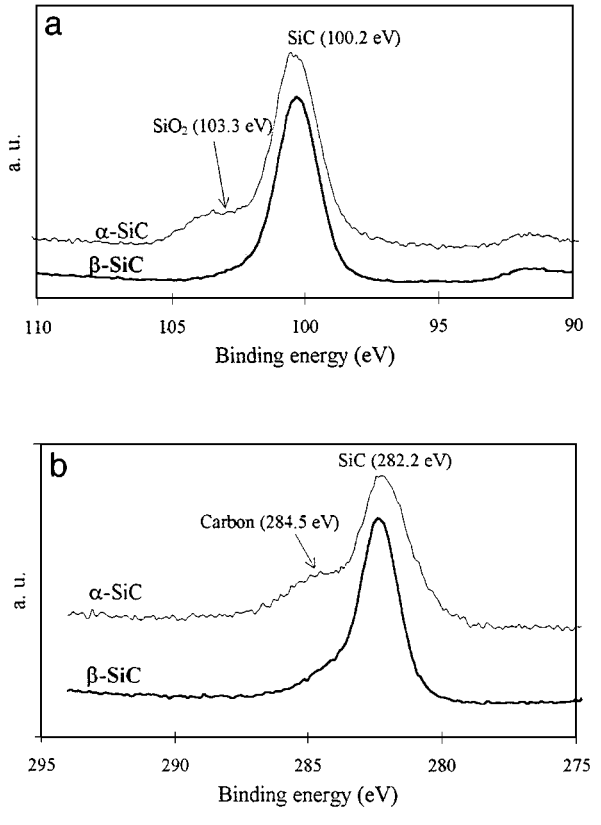

FIG. 1. XPS analysis of the supports: (1a) Si 2p level and (1b) C 1s level (Mg K X-ray source, ESCALAB 200R machine).

TABLE 3

Values of the Mean Diameter d of the Pd Particles, Determined by H_2 Thermodesorption and TEM, of the Three Considered Preparations

Activation treatment	Pd weight%	**d**(H_2) (nm)	**d**(TEM) (nm)
Ar (400°C)	1.05	10[a]	**d** ≈ 5
O_2 (350°C), H_2 (300°C)	1.14	56[b]	**d** ≈ 16
H_2 (400°C)	1.33	25	**d** ≈ 26

[a] Under only Ar treatment can some carbon residues be left on the surface; **d** determined from chemisorption measurements has to be considered cautiously.

[b] The O_2 (350°C)–H_2 (300°C) decomposition treatment leads to the formation of Pd_2Si particles embedded in the support (see Fig. 5 and related discussion). Therefore, **d** determined from chemisorption measurements is overestimated.

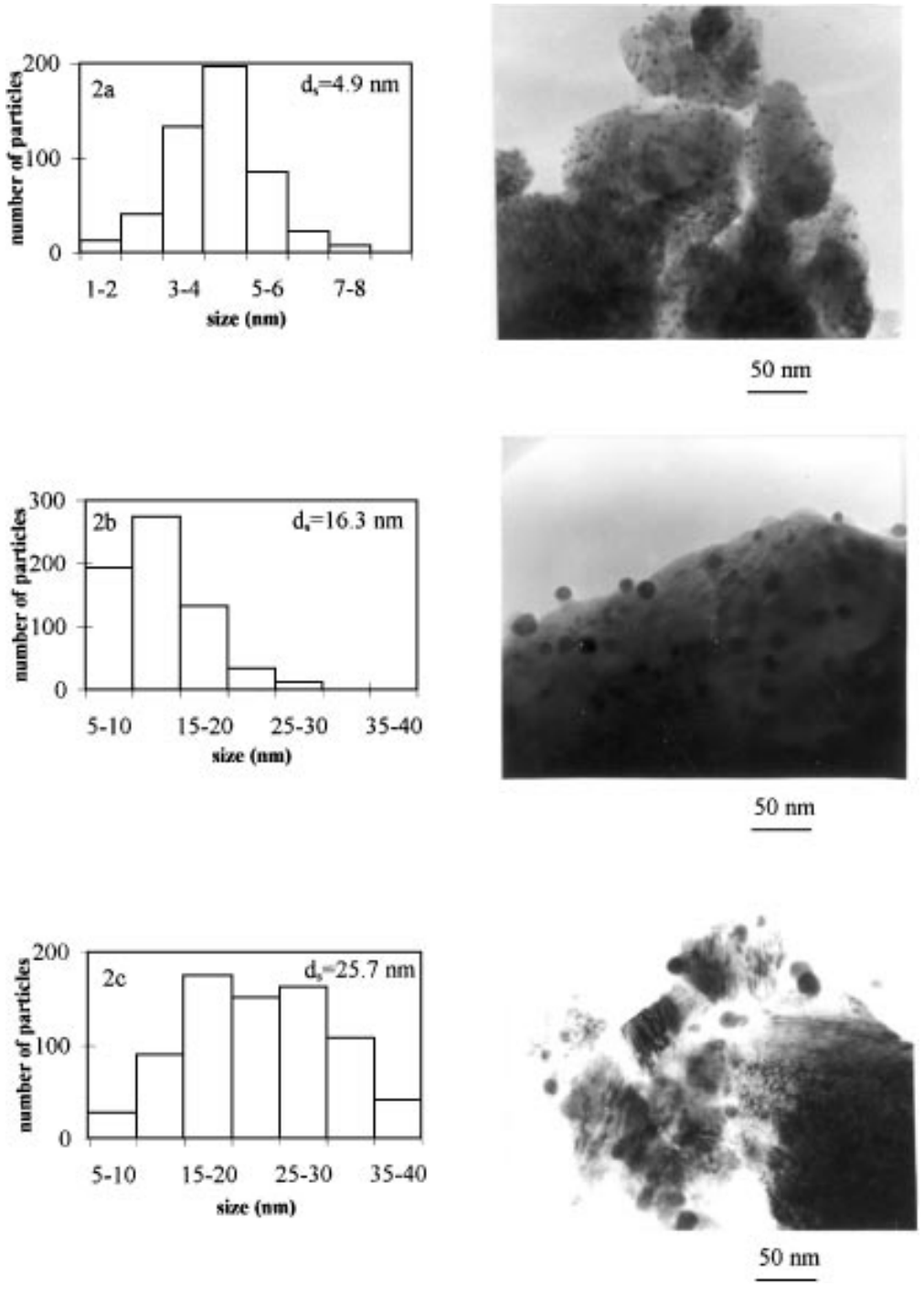

FIG. 2. TEM pictures and size distribution of the catalysts: (2a) Pd/β-SiC [Ar]; (2b) Pd/β-SiC [O_2–H_2]; (2c) Pd/β-SiC [H_2] (200 kV energy, JEOL 2010 microscope).

prepared by impregnation of silica with $Pd(AcAc)_2$, followed by decomposition under Ar flow where the presence of infrared bands ranging between 2800 and 3000 cm^{-1} characteristic of hydrocarbonated residues left on the metal surface are evidenced. Such species disappear after treatment under oxygen flow above 300°C (13).

The X-ray diffraction patterns of the different catalysts are reported in Fig. 3. The one for the β-SiC support is given for comparison (Fig. 3a).

The curves—CH_4 conversion versus temperature—are shown in Fig. 4. The light-off temperatures (at half conversion) are given in Table 4 for the samples having undergone

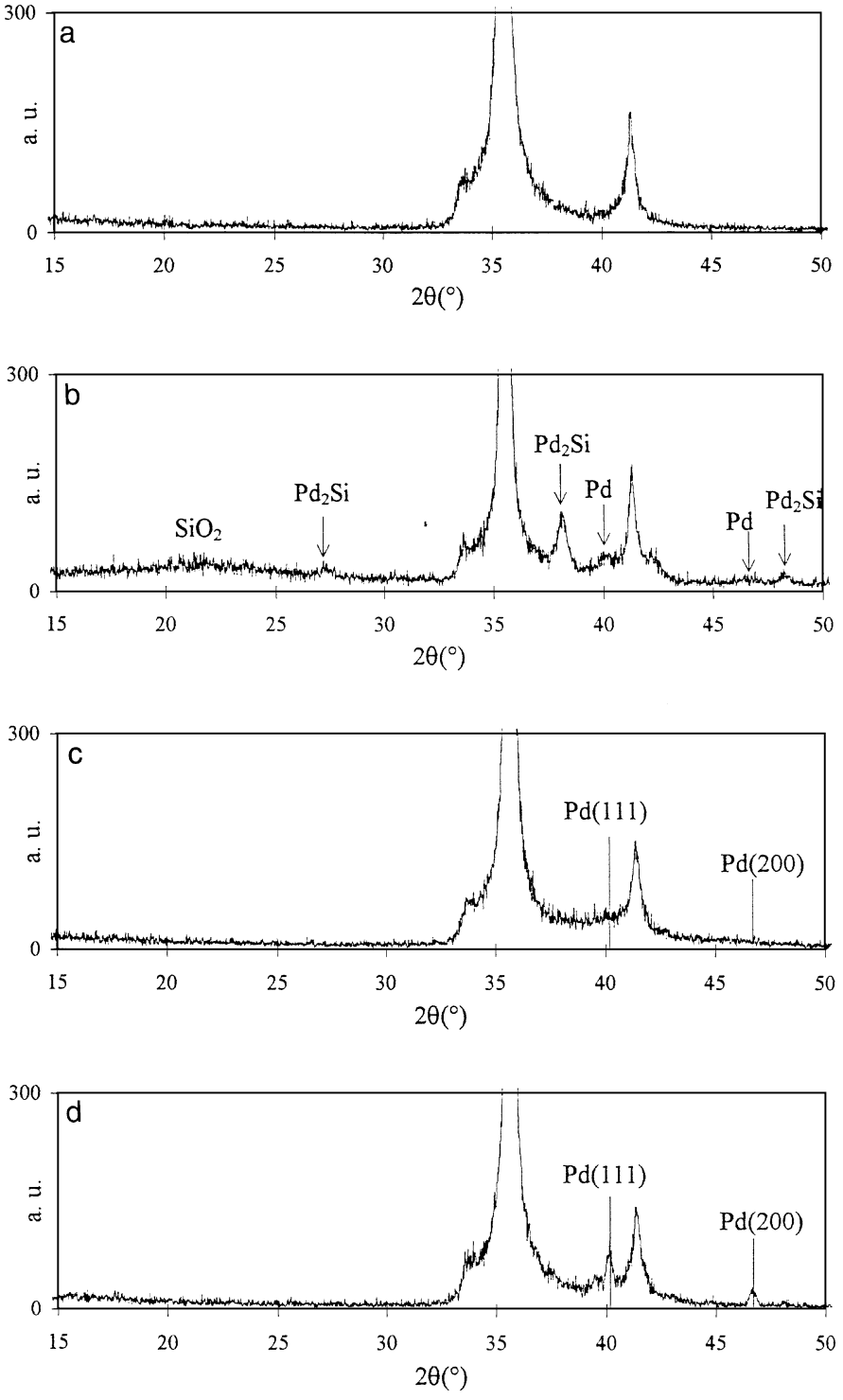

FIG. 3. X-ray diffraction patterns of the different catalysts: (3a) β-SiC; (3b) Pd/β-SiC [O_2–H_2]; (3c) Pd/β-SiC [Ar]; (3d) Pd/β-SiC [H_2].

the different activation treatments. Depending on the activation treatment, two catalytic behaviours are clearly observed. When the Pd complex is previously decomposed under argon atmosphere (Pd/β-SiC [Ar]), the catalyst is initially very active, but it is strongly deactivated after ageing under the reaction mixture up to 800°C (Fig. 4a). In reverse, when the precursors are previously decomposed under oxygen atmosphere and then reduced under H_2 (Pd/β-SiC [O_2–H_2]), or directly decomposed under hydrogen (Pd/β-SiC [H_2]), the catalysts show better thermal stability and their activity is not drastically decreased after ageing at 800°C (Figs. 4b and 4c).

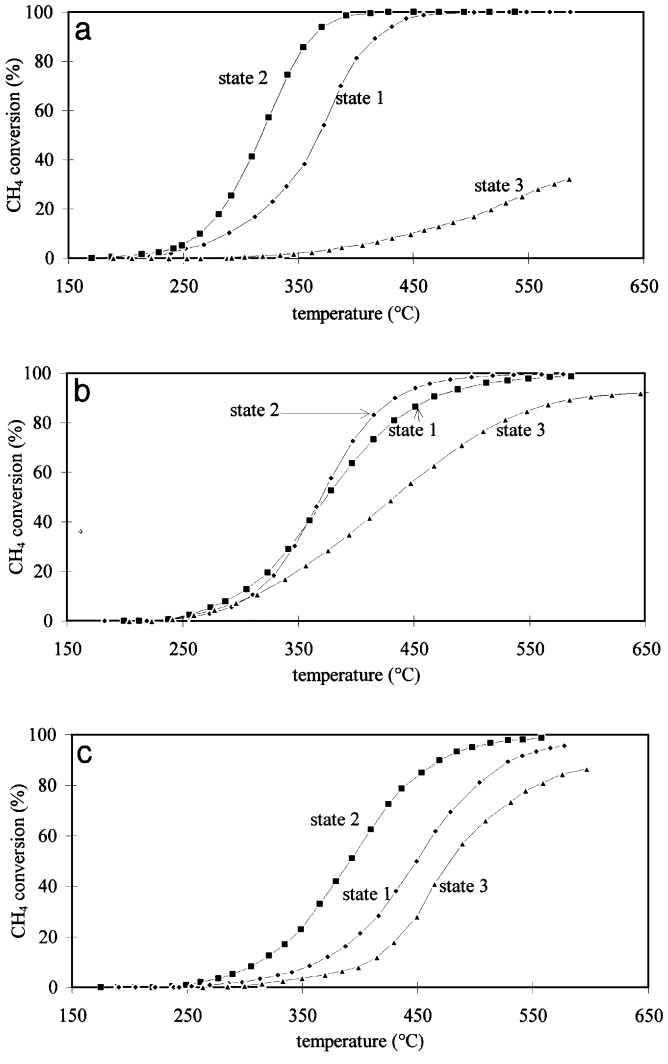

FIG. 4. Catalytic activities of the different catalysts with respect to the methane oxidation: (4a) on Pd/β-SiC [Ar]*; (4b) on Pd/β-SiC [O_2–H_2]**; (4c) on Pd/β-SiC [H_2]***. (* Precursor decomposed under Ar flow; ** precursor calcined under O_2 flow and reduced under H_2 flow; *** precursor treated only under H_2 flow.)

DISCUSSION

(a) Catalysts before Reaction

Let us first consider the X-ray diffraction patterns corresponding to the three considered catalysts shown in Fig. 3. For Pd/β-SiC [H_2] (Fig. 3d), the peaks characteristic of fcc Pd are well evidenced. They are narrow and well resolved. It may be concluded that the sizes of the Pd particles are very large, in agreement with the determination of the particle sizes by H_2 thermodesorption ($\mathbf{d} \approx 25$ nm) and TEM pictures (5 nm < diameter < 40 nm) (Fig. 2c).

For Pd/β-SiC [O_2–H_2] many X-ray lines characteristic of the hexagonal Pd_2Si phase are observed (Fig. 3c). Moreover, the X-ray peaks characteristic of fcc Pd are detected, but with a lower intensity than for the Pd/β-SiC [H_2] sample.

TABLE 4

Light-Off (Half-Conversion) Temperatures for the Considered Methane Oxidation on the Different Samples

Samples	State 1 (°C)	State 2 (°C)	State 3 (°C)
Pd/β-SiC (Ar)	370	330	Not reached (30% at 600)
Pd/β-SiC (O_2–H_2)	360	360	440
Pd/β-SiC (H_2)	450	390	475

On HR TEM pictures two kinds of particles characteristic of the sample are observed (Fig. 5). Many particles present (111) and ($\bar{2}21$) planes with an angle of around 64° and interplanar distances of respectively 0.236 and 0.217 nm, characteristic of the hexagonal structure of Pd_2Si (Fig. 5a). Such particles are surrounded by an amorphous SiO_x layer, formed during the preparation process. Other particles present families of (111) planes with an angle of around 70° and an interplanar distance of 0.225 nm, characteristic of fcc Pd (Fig. 5b). The Pd 3d binding energy, measured at 334.8 eV, is a little bit lower than that expected for Pd^0 (measured at 335.3 eV for massic Pd). In any case that value is largely lower than that corresponding to Pd_2Si, 336.8 eV (14), which is not (or rarely) detected. This agrees with the presence of both Pd particles and Pd_2Si particles covered by a SiO_x layer. Indeed, the percentage of analyzed Pd increases when the SiO_x layer is dissolved in the complex mixture HCl, nitric acid, and HF (Table 5). The Pd_2Si formation observed on Pd/β-SiC [O_2–H_2] at rather low temperatures could be due to a reaction occurring between Pd and the native silicon oxide layer occurring during the Pd complex decomposition under oxygen. The presence of a partially oxidized SiO_x species has been supposed to be a necessary step for such a Pd_2Si formation (15), which has been more generally observed for Pd deposited on SiO_2 under the H_2 reducing atmosphere at high temperature (16). The oxidation of the SiC support induced by the [O_2–H_2] activation treatment is clearly evidenced by the presence of a 103.3 eV photoelectric peak dominating in the Si 2p XPS spectrum (Fig. 6).

For Pd/β-SiC [Ar] only an increase of the background is measured in the X-ray diffraction pattern (Fig. 3b). It would correspond to the contribution to the spectrum of small

TABLE 5

Percentage of Analyzed Pd after Treatment with 2/3 HCl + 1/3 NO_3H (Only Not Encapsulated Pd is Analyzed) and after Treatment with 2/3 HCl + 1/3 NO_3H + HF (the Total Amount of Pd is Analyzed, Even Pd Encapsulated in Silica)

Samples	Percentage Pd analyzed 2/3 HCl + 1/3 NO_3H	Percentage Pd analyzed 2/3 HCl + 1/3 NO_3H + HF
Pd/β-SiC [Ar]	1.05	1.06
Pd/β-SiC [O_2–H_2]	0.27	1.14
Pd/β-SiC [H_2]	1.31	1.33

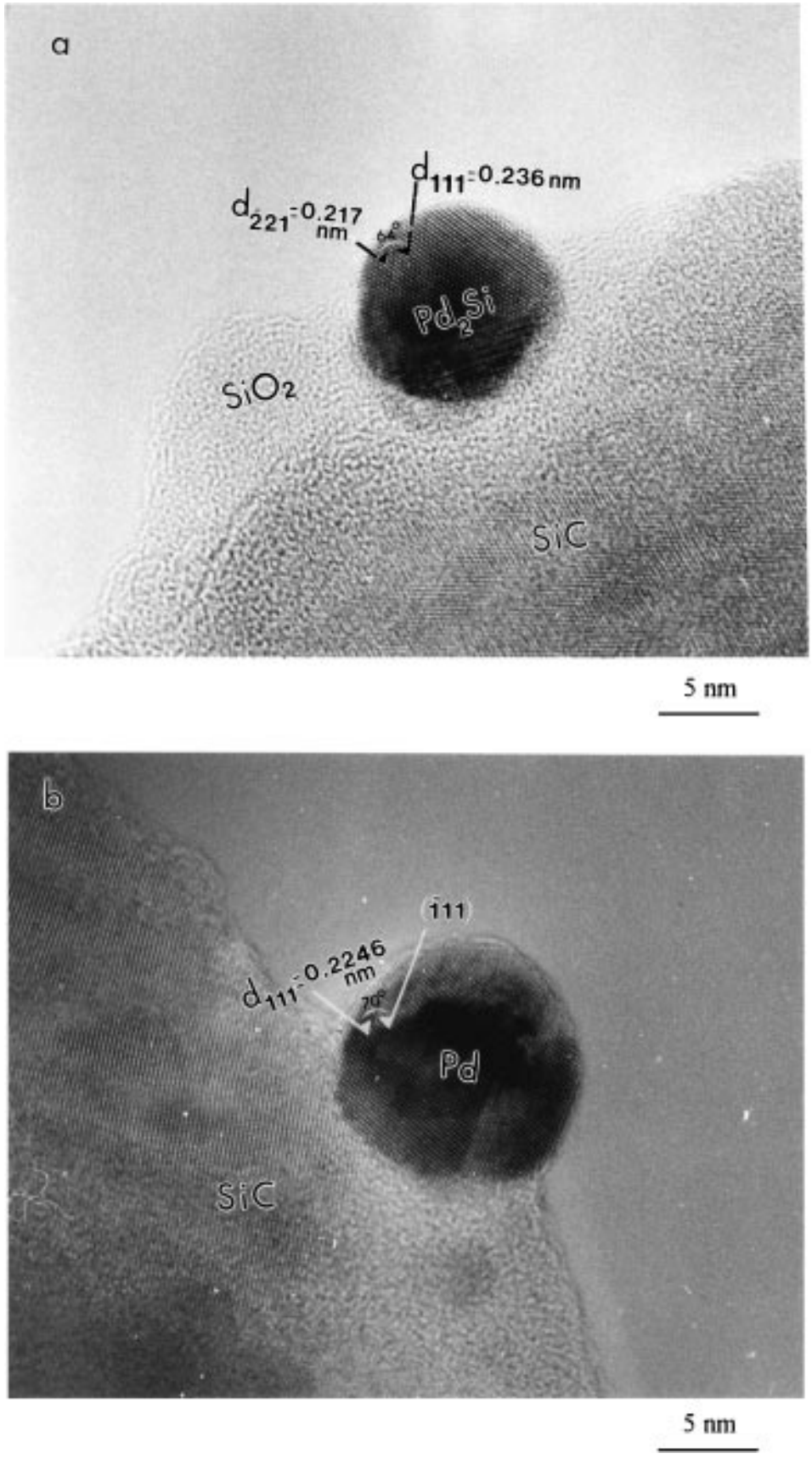

FIG. 5. HR TEM pictures of a Pd_2Si particle (5a) and of a Pd particle (5b) present on the Pd/β-SiC [O_2–H_2] catalyst. (200 kV energy, JEOL 2010 microscope).

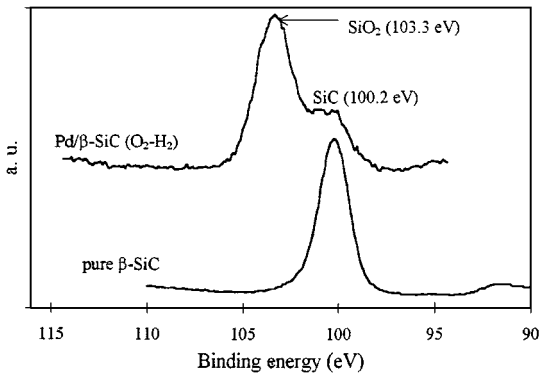

FIG. 6. Si 2p XPS spectrum of the Pd/β-SiC [O_2–H_2] catalyst (Mg K X-ray source, ESCALAB 200R machine).

Pd particles, as evidenced by TEM observations (Fig. 2a). The disagreement between particle size determination from TEM and H_2 chemisorption (Table 3) is due to some carbon residues left at the surface of the Pd particles inhibiting the hydrogen chemisorption as previously discussed.

(b) Catalysts after Reaction

With respect to the methane oxidation, an increase of activity is measured after a first reaction on Pd/β-SiC [Ar] and Pd/β-SiC [H_2] (Figs. 4a and 4c, state 2). Carbon residues, which are left on the surface due to the decomposition of the organic complexes (acetylacetonate) would be burnt after a first reaction under the oxidizing mixture ($CH_4/O_2 =$ 1/4); the activity increases then when a second reaction is performed. Such an increase of activity is not expected on the Pd/β-SiC [O_2–H_2] catalysts since it has been previously treated by O_2 during its preparation process, in agreement with the experimental results (Fig. 4b, state 2).

After ageing, a large decrease of activity is monitored on Pd/β-SiC [Ar] (Fig. 4b, state 3). This result would be explained, for a part by the increase of the Pd particle size, but which does not exceed 10 nm, and/or for the other part by the complete coating of the Pd particles by surface diffusion of some silicon oxide formed at high temperatures under the reaction mixture as shown on the HR TEM picture (Fig. 7). Surprisingly, such a large decrease of activity is not observed after ageing of Pd/β-SiC [O_2–H_2] and of Pd/β-SiC [H_2] (Figs. 4b and 4c, state 3). The analysis after ageing shows only a slight increase of the particle size while all the other properties of the sample are unchanged. It can be assumed that the encapsulation of Pd particles by SiO_x is made difficult because of the large size of the metal particles.

In any case a superficial oxidation of the SiC support is evidenced after reaction. Indeed, the 103.3 eV XPS line, characteristic of SiO_2, is then largely predominant in the Si 2p XPS spectra.

CONCLUSION

One can prepare Pd/β-SiC catalysts by impregnation of β-SiC support with the $(AcAc)_2$ Pd complex. The particle

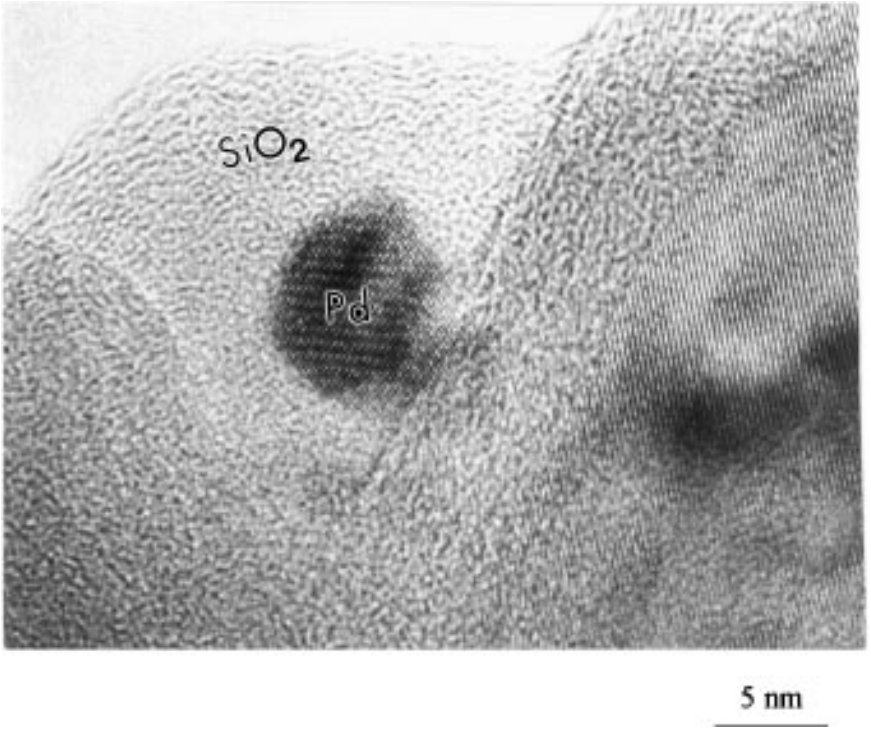

FIG. 7. HR TEM pictures of the Pd/β-SiC [Ar] catalyst after aging at 800°C.

size depends upon the activation treatment. A direct decomposition under argon atmosphere leads to small particles (**d** $\approx$ 5 nm). A decomposition of the impregnated $Pd(AcAc)_2$ precursor under oxygen or hydrogen forms larger particles (15–30 nm). Moreover, decomposition under oxygen generates the formation of a surface SiO_2 layer, and one evidences the formation of large Pd_2Si particles embedded in the SiO_x surface layer, together with large Pd particles.

These solids are active and selective for the complete oxidation of methane but their thermal stability, after ageing at 800°C under the reactional mixture, depends on their activation treatment. The Pd/β-SiC [Ar] catalyst is very active, but it completely deactivates after ageing under the reactional mixture at 800°C. This is due to the encapsulation of Pd particles in the SiO_x layer formed on the support. The Pd/β-SiC [O_2–H_2] and Pd/β-SiC [H_2] catalysts are less active, but they are more resistant to deactivation. Their better stability is explained by their larger Pd particle size.

ACKNOWLEDGMENT

The authors acknowledge the European Community for financial support through the Brite Euram Contract BRE2-CT94-0944.

REFERENCES

1. Vannice, M. A., Chao, Y. L., and Friedman, R. M., *Appl. Catal.* **20**, 91 (1986).
2. Ledoux, M. J., Hantzer, S., Cuong, P.-H., Guille, J., and Desaneaux, M. P., *J. Catal.* **114**, 176 (1988).
3. Boutonnet Kizling, M., Stenius, P., Anderson, S., and Frestad, A., *Appl. Catal. B Environ.* **1**, 149 (1992).
4. Lednor, P. W., *Catal. Today* **15**, 243 (1992).
5. Cuong, P.-H., Marin, S., Ledoux, M. J., Weibel, M., Ehret, G., Benaissa, M., Peschiera, E., and Guille, J., *Appl. Catal. B Environ.* **4**, 45 (1994).
6. Yamada, K., and Mohri, M., Silicon carbide (ceramics) *in* "Properties and Applications of SiC Ceramics."
7. Renouprez, A. J., Lebas, K., Bergeret, G., Rousset, J. L., and Delichère, P., *in* "Proceedings of the 11th International Congress on Catalysis" (J. W. Hightower, W. N. Delgass, E. Iglesia, and A. T. Bell, Eds.), Vol. 2, p. 1105, Elsevier, Amsterdam, 1996.
8. Parril, T. M., and Chung, Y. W., *Surf. Sci.* **243**, 96 (1991).
9. Zehringer, R., and Hauert, R., *Surf. Sci.* **262**, 21 (1992).
10. Dayan, M., *J. Vac. Sci. Technol. A* **3**, 361 (1985). [**4**, 38 (1986)]
11. Kaplan, R., *Surf. Sci.* **215**, 111 (1989).
12. Powers, J. M., and Somorjai, G. A., *Surf. Sci.* **244**, 38 (1991).
13. Trillat, J. F., Ph.D. thesis, Université Claude Bernard Lyon 1, 1997.
14. Juszczyk, W., and Karpinski, Z., *J. Catal.* **117**, 519 (1989).
15. Grunthaner, P. J., Grunthaner, F. J., and Madhukar, A., *J. Vac. Sci. Technol.* **20**, 680 (1982).
16. Lien-Lung Shew, Karpinski, Z., and Sachtler, W. M. H., *J. Phys. Chem.* **93**, 4890 (1989).